

Characteristics of Sealed-Off Waveguide CO₂ Lasers

RICHARD L. ABRAMS AND WILLIAM B. BRIDGES

Abstract—Gain and output power of sealed-off waveguide CO₂ lasers are presented as a function of gas mixtures and total gas pressure. Experimental data on circular-bore and square-channel waveguide lasers are presented. Output power per unit length of 0.2 W/cm is achieved for both types of lasers in agreement with gas-discharge scaling laws which are presented. Saturation intensities as high as 24 kW/cm² are inferred from the data. The effects of the optical properties of the waveguide wall material on the waveguide losses are discussed and theoretical waveguide loss versus wavelength is presented for BeO, Al₂O₃, and fused silica.

I. INTRODUCTION

THE CONCEPT of a hollow waveguide gas laser was first suggested by Marcatili and Schmeltzer [1] and later demonstrated by Steffen and Kneubuhl [2] and Smith [3]. In addition, CO₂ waveguide lasers employing flowing gas have recently been demonstrated [4]–[6]. The reduction in discharge tube diameter and the corresponding increase in gas pressure inherent in waveguide lasers has resulted in CO₂-laser operation at gas pressures in excess of 300 torr. This implies a pressure-broadened gain linewidth in excess of 1500 MHz, where frequency tuning [7] and mode-locking experiments [8] become very attractive. In particular, a CO₂ laser tunable over 1500 MHz would be useful as a local oscillator in a Doppler tracking receiver for satellite communications.

In this paper we discuss what may be expected as the CO₂ laser is scaled to smaller discharge diameters using the tube wall as an optical waveguide and report on our measurements of gain, output power, and efficiency in sealed-off CW capillary-bore CO₂ lasers. A section is also included on the losses encountered in hollow dielectric waveguides, including theoretical results for several possible guiding materials.

II. PLASMA SCALING

Waveguiding allows us to extend measurement of laser medium characteristics to smaller diameter discharges without being limited by the high optical losses that would attend simple free-space diffraction-limited wave propagation in such tubes. In this section we review briefly what is to be expected from theory for the variation of gain, saturation flux density, efficiency, etc., with changes in tube parameters.

Manuscript received March 30, 1972. The research reported in this paper was sponsored in part by the Air Force Cambridge Research Laboratories, Air Force Systems Command, under Contract F19628-73C-0086. The paper does not necessarily reflect endorsement by the sponsor.

The authors are with Hughes Research Laboratories, Malibu, Calif. 90265.

TABLE I
SIMILARITY RELATIONS

Quantity	Relation
Gas Temperature T_g	$T_{g2} = T_{g1} \quad (1)$
Gas number density N	$D_2 N_2 = N_1 D_1 \quad (2)$
Gas pressure p	$p_2 D_2 = p_1 D_1 \quad (3)$
Electron temperature T_e	$T_{e2} = T_{e1} \quad (4)$
Electron density N_e	$N_{e2} D_2 = N_{e1} D_1 \quad (5)$
Current Density J	$J_2 D_2 = J_1 D_1 \quad (6)$
Current I	$I_2 / D_2 = I_1 / D_1 \quad (7)$
Electric field E	$E_2 D_2 = E_1 D_1 \quad (8)$
DC resistance Z	$Z_2 D_2^2 = Z_1 D_1^2 \quad (9)$
Power input/length P_i / L	$P_{i2} / L = P_{i1} / L \quad (10)$
Gain coefficient α	$\alpha_2 D_2 = \alpha_1 D_1 \quad (11a)$
	$\alpha_2 = \alpha_1 \quad (11b)$
Saturation flux density S	$S_2 D_2 = S_1 D_1 \quad (12a)$
	$S_2 D_2^2 = S_1 D_1^2 \quad (12b)$
Power output/volume P_o / V	$(P_{o2} / V) D_2^2 = (P_{o1} / V) D_1^2 \quad (13)$
Power output/length P_o / L	$P_{o2} / L = P_{o1} / L \quad (14)$
Efficiency η	$\eta_2 = \eta_1 \quad (15)$

Konyukhov [9] has given perhaps the most logical development of the similarity laws applicable to CO₂ lasers. The net results are essentially the same as the well-known relations for similar gas discharges, i.e., discharges in which the electron temperature is the same, as given by von Engel and Steenbeck [10] for gas discharges, and extended to He-Ne lasers by White and Gordon [11]. Konyukhov, however, has considered the added scaling problems introduced by including a finite gas temperature—an important parameter in molecular lasers. He has shown that if the gas temperatures, as well as the electron temperatures, are the same at corresponding points in two discharges, then the earlier similarity relations for zero-temperature gases [10], [11] hold. These relations are summarized in Table I for two discharges of diameters D_1 and D_2 . Relations (1)–(10) involve only the discharge parameters, while the remaining relations also involve optical interactions. Relations (11) and (12) are given for both Doppler- and pressure-broadened lines, and require an additional comment. Konyukhov gives only the Doppler-broadened form, but since we are interested in high-pressure operation in the smaller diameter

tubes, the pressure-broadened case must be used instead. The relations for the Doppler-broadened case (11a), (12a) follow directly from the relation for gas density (2) and the observation [9] that the relative populations of all levels remain the same in similar discharges, provided the gas-temperature distribution is held constant. The gain expression (11a) assumes the laser transition linewidth is constant. However, at high pressures (greater than 20 torr or so), the linewidth is also proportional to the number density, so that the gain becomes independent of N and hence independent of D (11b). Likewise, for the saturation parameter S , the linewidth of the transition is broadened proportionally by collisions so that an additional variation with N , and hence D , results (12b). Relation (13) assumes an essentially homogeneous interaction such that the power per unit volume is given by the product αS . This relation is well satisfied for homogeneously broadened lines, e.g., pressure broadened, and is approximately true for the well-saturated multimode operation which "burns off the top" of an inhomogeneously broadened line [12]. Relation (14) assumes that the optical mode always fills the entire diameter D —a condition automatically satisfied in the waveguide laser.

We should emphasize that the relations given in Table I describe *similar* discharges; that is, if the independent parameters of the two discharges are adjusted to satisfy the conditions given in Table I, then the remaining parameters should also satisfy the relations listed. A convenient choice of independent parameters is T_g , p , and I . The remaining variables may then be considered as dependent characteristics. Note that Table I does *not* tell us, for example, how the output power varies with gas pressure for a given tube; rather, the relations tell us only how the output powers of two *similar* tubes will compare [according to relation (14) they will be the same]. Let us suppose that the optimum conditions have been determined for a particular tube. The relations given in Table I will then give us the optimum conditions for similar tubes of different diameters. Table I tells us immediately several interesting things about waveguide lasers, compared to larger diameter lasers. As the tube diameter is made smaller,

- 1) the pressure increases;
- 2) the tube current decreases;
- 3) the tube voltage increases;
- 4) the gain remains the same;
- 5) the power output per unit length remains the same;
- 6) the efficiency remains the same.

Of course, the above assumes that the optical losses are independent of the discharge tube diameter. This assumption is less true for smaller diameters in a waveguide laser than for a conventional laser.

It is also clear from Table I why power output per unit volume is *not* useful as a scaling parameter in the same sense as it is used in TEA lasers, for example. High values of P/V obtained from small-diameter lasers cannot be

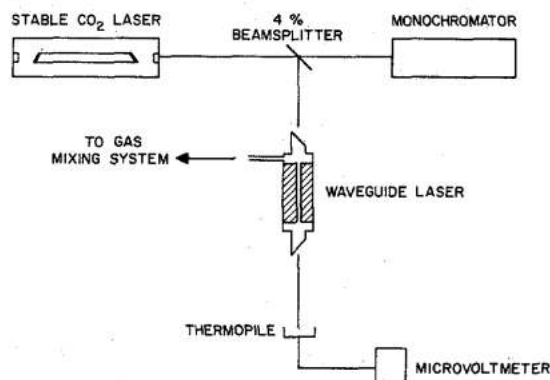


Fig. 1. Experimental arrangement for measurement of waveguide laser gain.

scaled to large volumes. Power per unit length is the proper quantity for scaling waveguide CO₂ lasers (or for that matter, all wall-cooling-dominated CO₂ lasers).

III. EXPERIMENTAL RESULTS

Our experimental effort was geared to measurements of the parametric dependence of laser gain on gas mixture and total pressure for sealed-off capillary-bore tubes. Detailed measurements of the laser gain for He:CO₂ gas mixtures were made, and then the effects of N₂ and Xe gas additives were measured for selected mixtures. Particular attention was paid to the effects of N₂ and Xe on discharge voltage and stability. Finally, measurements of the output power and efficiency were made on an 18-cm × 1.5-mm ID BeO laser tube as a function of gas mixtures and total pressure. In addition, we present power output and efficiency data on a 7.5-cm CO₂ laser with a 1.5-mm *square* capillary bore.

A. Gain Measurements

The experimental arrangement for measurement of gain is shown in Fig. 1. A sealed-off stable CO₂ laser, tuned to the center of the $P(20)$ 10.6- μ m transition, was used as an input signal to the capillary-bore laser. The output was detected with a thermopile. Gain measurements were made by observing the transmitted power with the amplifier discharge on and off. Care was taken that the absorption at 10.6 μ m by the cold gas, as well as detected fluorescence from the discharge, were negligible factors in these measurements. We also assured ourselves that the amplifier gain was measured in the linear region by using only a few milliwatts of input power. For each series of measurements, the appropriate gases were thoroughly mixed in a separate chamber, and then the mixture was metered into the amplifier tube. In this manner, gain measurements were made as a function of gas mixture and total pressure.

Fig. 2 shows the details of the narrow bore tube used in these experiments. An all-metal ceramic construction with low-loss CdTe Brewster windows was selected. A water-

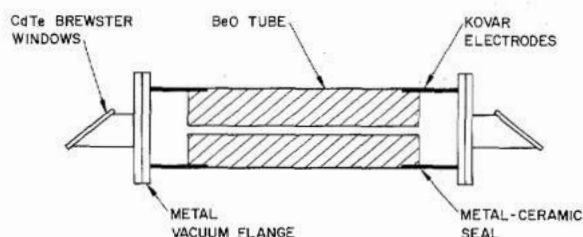
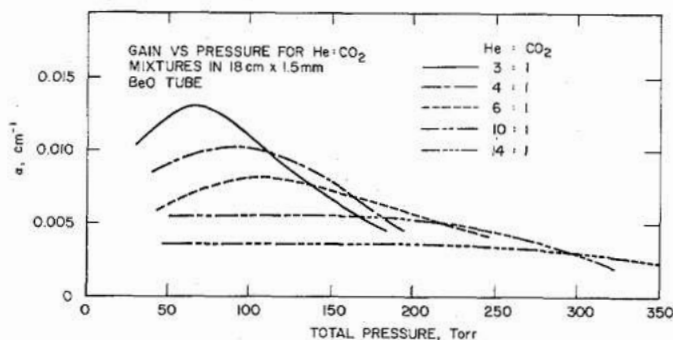


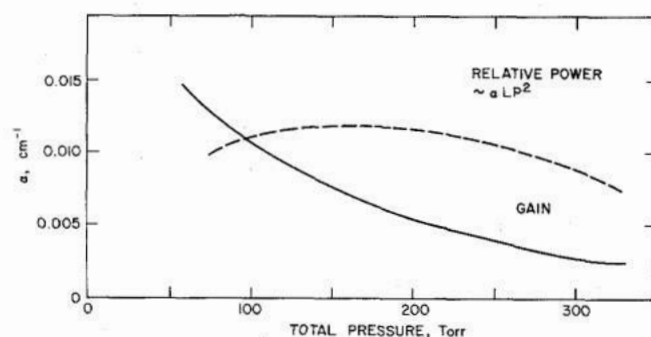
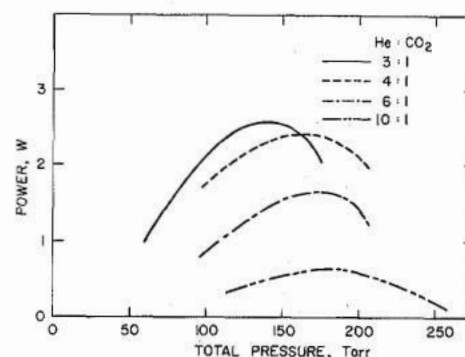
Fig. 2. Construction details of BeO capillary bore laser.

Fig. 3. Gain versus total pressure for various sealed-off He : CO₂ mixtures in an 18-cm \times 1.5-mm BeO tube.

cooled aluminum clamp near the cathode was sufficient to maintain the temperature of the high thermal conductivity BeO tube constant within 10°C along the bore length. The temperature drop radially across the BeO bore wall is calculated to be less than 0.5°C. For the gain measurements reported here, an 18-cm \times 1.5-mm ID discharge tube was employed.

The measured gain as a function of total pressure is shown in Fig. 3 for several CO₂:He mixtures. The current was held at 3.0 mA for these measurements. However, the gain was nearly independent of discharge current from 2 to 5 mA. For mixtures rich in CO₂, the gain peaks at lower pressures. As the He concentration is increased, the peak gain moves to higher pressures, but has a lower value. Mixtures which have very little CO₂, e.g., 14:1, show a gain almost independent of pressure, implying that the inversion ratio is also independent of pressure for these mixtures. If one wishes to extract the maximum amount of power from the laser, the saturation parameter must also be considered. At low discharge currents, and for homogeneous broadening, the saturation parameter increases as p^2 , so the available power goes as αp^2 , where α is the small-signal gain. Fig. 4 shows the peak gain α_{\max} (i.e., the envelope of the Fig. 3 curves) and also $\alpha_{\max} p^2$ versus pressure. If cavity losses can be kept small compared with gain, it is clear that significant power output should be available at pressures above 300 torr.

We have added N₂ and Xe to selected He : CO₂ mixtures. In general, we find that 0.25–0.50 parts of N₂ and 0.25 parts of Xe give the maximum gain improvement, but this improvement only amounts to a 10-percent increase in gain above the curves shown in Fig. 3. Xe has the effect of decreasing the discharge potential, while N₂ has the opposite effect.

Fig. 4. Maximum available gain for He : CO₂ mixtures and expected relative available power versus total pressure for He : CO₂ mixtures in 18-cm \times 1.5-mm BeO tube.Fig. 5. Output power versus total pressure for He : CO₂ mixtures in 18-cm \times 1.5-mm BeO tube.

B. Power Output

We have made power output measurements with a variety of gas mixtures and pressures for the 18-cm \times 1.5-mm ID tube discussed above, as well as for a 7.5-cm \times 1.5-mm square tube (which, because of its construction, we call a *channel laser*). These results are discussed separately.

Circular Waveguide Laser: The 18-cm \times 1.5-mm ID BeO tube was inserted into a resonator¹ formed by a 23-cm radius-of-curvature total reflector spaced 22 cm from one end of the laser and a 14-cm radius-of-curvature 95-percent reflecting mirror positioned 10 cm from the opposite end. Laser output power versus total pressure for the various He : CO₂ mixtures is shown in Fig. 5. The peak laser output clearly occurs at pressures well above the optimum pressure for peak gain, demonstrating the effect of increasing saturation parameter with pressure. Fig. 6 shows the pressure dependence of laser voltage and efficiency for the various He : CO₂ mixtures. The laser current was set to 3.0 mA for these measurements.

We have seen that high-pressure operation can be realized with He-rich mixtures and that discharge voltage can be reduced by adding Xe. In Fig. 7 the laser output power and discharge voltage versus total pressure is shown for an He : CO₂ : Xe mixture of 14 : 1 : 0.25. The maximum power is reduced because the gain is reduced to the

¹ The design of optimum resonators for waveguide lasers is discussed in the papers by Abrams [13] and Chester and Abrams [14].

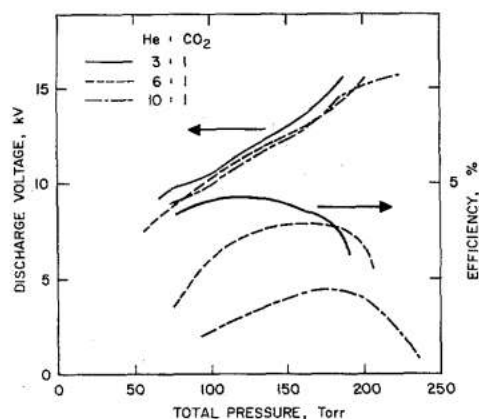


Fig. 6. Discharge voltage and laser efficiency versus total pressure for He:CO₂ mixtures in 18-cm \times 1.5-mm BeO tube.

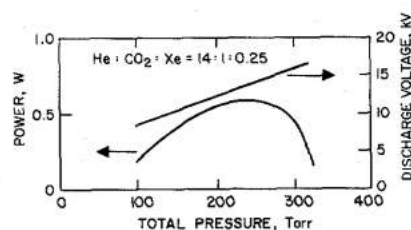


Fig. 7. Laser output power and discharge voltage versus total pressure for mixture of He:CO₂:Xe = 14:1:0.25. For these measurements, laser output mirror reflectivity is 98 percent.

point where losses are important, but laser action is demonstrated out to 320 torr. For these latter measurements, the 95-percent mirror was replaced with a 98-percent reflecting mirror with the same radius of curvature.

Recent measurements with the same laser using higher quality CdTe windows gave a power output of 4.0 W at 150 torr with a gas mixture of He:CO₂:N₂:Xe = 4:1:0.5:0.25. Under these conditions, the laser efficiency was 7.1 percent, comparing favorably with larger diameter tubes of the same gain as we expect from the scaling laws. This corresponds to a power per unit length of 0.22 W/cm of length.

Channel Laser: Hollow waveguide lasers may also be operated in noncircular guides. In particular, we have experimented with square waveguides machined in Al-300 alumina. The advantages of this structure include ease of manufacture and a convenient geometry for internal modulator applications. A photograph and exploded view of such a 7.5-cm-long channel laser are shown in Fig. 8. One mirror is totally reflecting and the other has 3-percent transmission. The mirrors are both flat. The center electrode is hollow and acts both as a cathode and gas-filling port. The pins at either end are the anodes.

The output power versus total pressure for several He:CO₂ gas mixtures in the 3-in channel laser is shown in Fig. 9. With a mixture of He:CO₂:N₂:Xe = 4:1:0.5:0.25, an output power of 1.4 W at 6-percent efficiency was obtained at 150 torr and 0.3 W was observed at 350 torr. Thus a power per unit length of 0.19 W/cm was achieved. This compares with 0.22 W/cm obtained

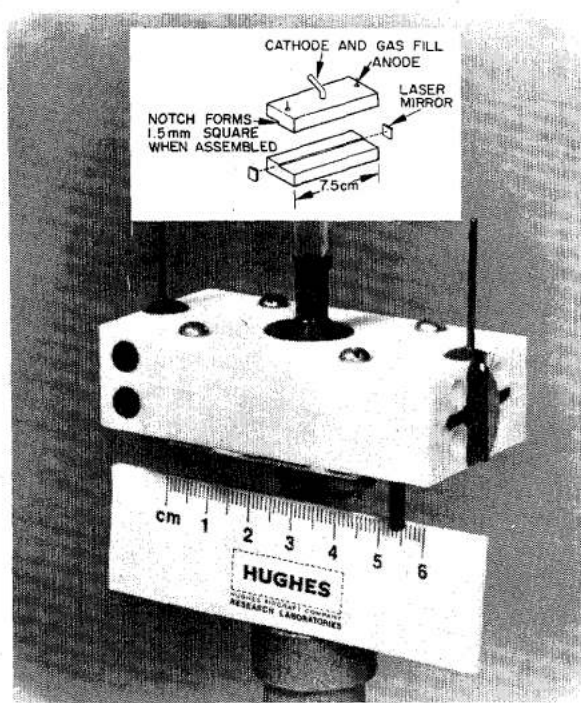


Fig. 8. Photograph and exploded view of 3-in 1.4-W channel laser.

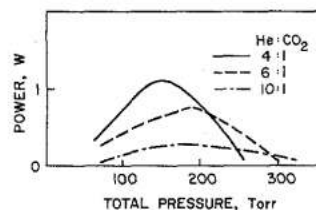


Fig. 9. Laser output power versus total pressure for He:CO₂ mixtures in 7.5-cm channel laser.

from the longer 18-cm \times 1.5-mm ID laser. For comparison, Deutsch and Horrigan [15] reported 0.6 W/cm from a sealed-off CO₂ laser, 1 m \times 20 mm ID. There are several reasons for the difference, as follows.

1) Their laser is 1 m long, and thus has sufficient gain to operate far above threshold. Our waveguide lasers also have finite guiding loss which has not been included in the scaling relationships.

2) Their laser output mirror was carefully optimized for maximum power, while ours was not.

3) The scaling laws are probably not exactly obeyed over a 10:1 variation in tube dimensions. For example, it is unlikely that the electron temperature or even the electron distribution will remain exactly the same over a wide range of dimensions, especially if the dimensions approach the wall sheath size.

Bridges *et al.* [4] reported on a flowing CO₂ waveguide laser made from a 12.5-cm-long \times 1.0-mm ID Pyrex tube. For optimum output coupling they obtained 0.9 W at room temperature. This gives a power per unit length of 0.07 W/cm. In principle, the flowing laser should produce greater output than our sealed-off tubes. However, it is likely that the low thermal conductivity in Pyrex results in a higher discharge temperature. In addition, the pressure

gradients present in the flowing tubes result in less than optimum discharge conditions. It is interesting that, although their measured gain of 24 dB/m at room temperature ($= 0.055 \text{ cm}^{-1}$) is much greater than our measured value of $\sim 0.01 \text{ cm}^{-1}$, we observe three times their power per unit length. This is presumably due to our higher and more uniform operating pressure.

C. Saturation Parameter

The saturation intensity in CO_2 lasers can be increased by molecule-molecule collisions, by electron-molecule collisions, and by diffusion of molecules into the active region [16]. At the high pressures used in our experiments, it is expected that the molecule-molecule collisions would dominate, as they scale as the square of the operating pressure. The highest saturation parameters reported with conventional CO_2 lasers is 100 W/cm^2 at about 10-torr pressure [17]. At a pressure of 150 torr, this scales to 22.5 kW/cm^2 , assuming a (pressure)-squared variation.

We can estimate the saturation flux I_0 from output power data in the sealed-off 18-cm \times 1.5-mm ID laser. We assume an average intensity $I = P/\pi w^2$, where P is the internal laser power and w is the e^{-1} intensity radius of the Gaussian beam which best matches the EH_{11} waveguide mode [13]. This gives a value of $w/a = 0.455$. From our estimated guiding and mirror losses (total loss/pass is 4 percent) and our known mirror transmission and gain, we calculate a saturation flux of 24 kW/cm^2 for a 4.0-W output at 150 torr. This is a reasonable value if a pressure-squared sealing law is assumed.

The gain data from Fig. 3 and the output power data of Fig. 5 have been combined to calculate the saturation intensity versus total pressure for several He : CO_2 mixtures. A log-log plot of the results is shown in Fig. 10. The solid lines have a slope of 2 representative of a square law dependence. It is clear that the assumed pressure-squared dependence of the saturation intensity is a good approximation for these experiments.

Bridges *et al.* [4] found a saturation intensity of 2100 W/cm^2 at room temperature at an average pressure of 100 torr. This is considerably less than one would expect from the simple scaling mode. However, they had a large pressure drop across the tube (140 torr), and it is likely that their large gain occurred at the low-pressure end where the saturation flux would be lower. If one assumes the p^2 variation, then an effective pressure of $10 \cdot (2100/100)^{1/2} = 46 \text{ torr}$ is implied. It is quite possible that in the presence of the pressure gradient, the average pressure of 150 torr is not the appropriate measure. This effect would also explain their relatively low efficiency and power per unit length.

It is interesting to speculate on the available power per unit length if waveguide and other losses are negligible in waveguide lasers. The available power per unit length is given by

$$P/L = \pi w^2 \alpha I_0$$

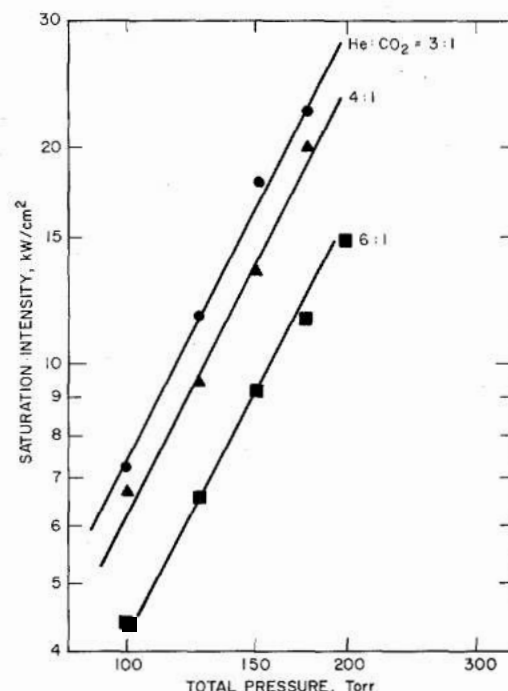


Fig. 10. Saturation intensity, as calculated from the data in Figs. 3 and 5, versus total pressure for several He : CO_2 mixtures.

where w is the $1/e$ intensity radius, α is the unsaturated small-signal gain, and I_0 is the saturation flux. Assuming $\alpha = 0.01 \text{ cm}^{-1}$, $I_0 = 25 \times 10^3 \text{ W/cm}^2$, $w = 0.455 \text{ A}$, and a 1.5-mm ID tube

$$P/L = 0.9 \text{ W/cm}$$

which is in reasonable agreement with the sealed-off values reported by Deutsch and Horrigan, as predicted from our scaling laws. Note that the constancy of gain and power per unit length with tube radius could also have been used to estimate the saturation flux for waveguide gas lasers, but the same value would be obtained.

D. Waveguide Losses

Thus far we have ignored waveguide losses in discussing scaling laws and experimental performance, and we now consider them. Marcatili and Schmeltzer [1] give the dielectric waveguide loss coefficient for the nm th mode as

$$\alpha_{nm} = \left(\frac{u_{nm}}{2\pi} \right)^2 \frac{8\lambda^2}{D^3} \text{Re}(\nu_n) \quad (1)$$

where u_{nm} is the m th root of J_{n-1} and ν_n is an expression involving the complex index of refraction of the wall material $\nu = n - ik$:

$$\nu_n = \frac{\frac{1}{2}(\nu^2 + 1)}{(\nu^2 - 1)^{1/2}} \quad (2)$$

for the EH_{nm} modes. Marcatili and Schmeltzer evaluated (1) for a visible laser ($0.6328 \mu\text{m}$) with lossless glass walls

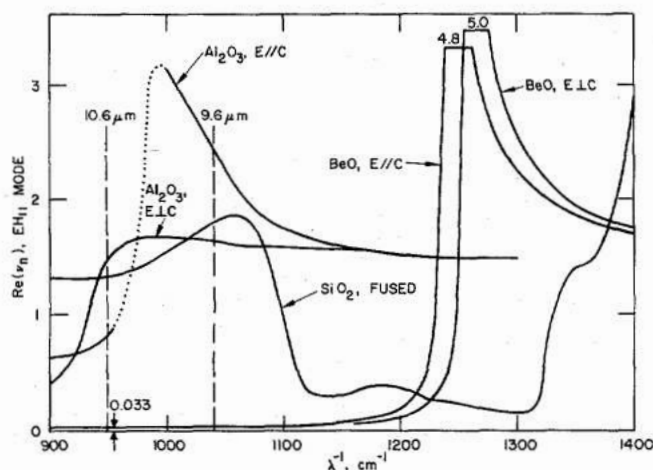


Fig. 11. Refractive-index dependent contribution to the waveguide loss $\text{Re}(\nu_n)$ of the EH_{11} mode shown as a function of frequency for Al_2O_3 , SiO_2 , and BeO . Curves for Al_2O_3 and BeO show two orientations with respect to the c axis.

($n = 1.5$, $k = 0$), obtaining 1.85 dB/km for a 2-mm-diam waveguide.

The situation is much different at 10.6 μm , since all practical laser bore materials are quite lossy (k large). However, a lossy wall material does not necessarily mean that the waveguide loss α_{11} will be large. In fact, some examination of (2) for complex ν will show that very large values of k or n will result in small values of $\text{Re}(\nu_n)$, and hence α_{11} . A simple way of picturing this physically is to think of the penetration of the guided wave into the wall material and to note that very high dielectric constants (large n) or very high conductivity (large k) will tend to exclude the fields from the dielectric, i.e., the wave is efficiently reflected back into the hollow guide by the wall.

It is interesting to put in numerical values for the optical constants n and k for those materials that are usually used to make practical discharge tube bores— Al_2O_3 , SiO_2 , and BeO . The result for $\text{Re}(\nu_n)$ is plotted in Fig. 11. Note that there is substantial variation in waveguide loss from material to material, and also quite a variation with wavelength. In fact, by choosing a material which exhibits the proper variation with wavelength, one could conceivably use the waveguide loss to select laser transitions. For example, SiO_2 has a somewhat higher loss at 9.6 μm than at 10.6 μm , and substantially lower loss at 8 μm . Variations in n and k occur near material resonances, so that dielectrics with resonances near the desired laser wavelength should be investigated for wavelength selective properties. Unfortunately, experimental values of optical constants are only known for a limited number of materials suitable for waveguide walls. The values used to plot Fig. 11 were taken from Šimon and McMahon [18] for SiO_2 , Loh [19] for BeO , and Häfele [20] for Al_2O_3 . Since the data for BeO and Al_2O_3 were for single-crystal material, curves for two different crystal orientations are shown. The actual values for polycrystalline material could reasonably be expected to lie somewhere between the two curves shown.

Using (1) and the data from Fig. 10, we have

$$\alpha_{11} = \begin{cases} 4.3 \times 10^{-5} \text{ cm}^{-1}, & \text{for BeO} \\ 1.8 \times 10^{-3} \text{ cm}^{-1}, & \text{for SiO}_2 \end{cases} \quad (3)$$

for a 1-mm-diam waveguide at 10.6 μm . A BeO tube would have negligible waveguide loss compared to a laser medium gain of 0.01 cm^{-1} , while the SiO_2 tube has a loss equal to ~ 17 percent of the gain. Doubling the diameter to 2 mm decreases the waveguide losses by a factor of 8, so that both materials have negligible loss. Reducing the diameter by one-half to 0.5 mm would increase the SiO_2 loss to 0.014 cm^{-1} so that the tube would not oscillate with a medium gain of 0.01 percent.

It would seem from Fig. 11 and from thermal properties that BeO is the ideal material for a 10.6- μm waveguide laser. However, the curve shown is based on single-crystal measurements, and may not be typical of the quality of material used in ceramics. An even more serious reservation is that no accounting has been made of the losses caused by scattering from grain boundaries in the polycrystalline ceramic or the finite surface roughness left by the grinding process. In these respects, SiO_2 capillary tubing is superior. The truly optimum choice awaits further experimental measurement of these contributions.

IV. CONCLUSIONS

We have reported here the first experimental results on sealed-off capillary-bore CO_2 lasers. Significant output power has been achieved at pressures in excess of 300 torr, and we observe efficient laser output in the 150–200-torr region. Power outputs per unit length of ~ 0.2 W/cm have been achieved in an 18-cm \times 1.5-mm ID circular waveguide laser, as well as in a 7.5-cm \times 1.5-mm square channel laser. The saturation parameter and output power are in reasonable agreement with estimates from simple scaling-law arguments. Waveguide loss calculations for SiO_2 , Al_2O_3 , and BeO guides have been presented.

Hollow dielectric waveguides have permitted us to extend the operation of sealed-off CO_2 lasers to smaller tube diameters and correspondingly higher operating pressures. The further development of this technique promises a class of CO_2 -laser devices which are efficient, small, and tunable over bandwidths in excess of 1 GHz.

ACKNOWLEDGMENT

The authors wish to thank O. P. Judd for valuable technical discussions and R. E. Brower for expert technical assistance.

REFERENCES

- [1] E. A. J. Marcetili and R. A. Schmeltzer, "Hollow metallic and dielectric waveguides for long distance optical transmission and lasers," *Bell Syst. Tech. J.*, vol. 43, pp. 1783–1809, July 1964.
- [2] H. Steffen and F. K. Kneubuhl, "Dielectric tube resonators for infrared and submillimeterwave lasers," *Phys. Lett.*, vol. 27A, pp. 612–613, Sept. 1968.

- P. Schwaller, H. Steffen, J. F. Moser, and F. K. Kneubühl, "Interferometry of resonator modes in submillimeter wave lasers," *Appl. Opt.*, vol. 6, pp. 827-829, May 1967.
- [3] P. W. Smith, "A waveguide gas laser," *Appl. Phys. Lett.*, vol. 19, pp. 132-134, Sept. 1971.
- [4] T. J. Bridges, E. G. Burkhardt, and P. W. Smith, "CO₂ waveguide lasers," *Appl. Phys. Lett.*, vol. 20, pp. 403-405, May 1972.
- E. G. Burkhardt, T. J. Bridges, and P. W. Smith, "BeO capillary bore CO₂ waveguide laser," *Opt. Commun.*, vol. 6, pp. 193-195, Oct. 1972.
- [5] R. E. Jenson and M. S. Tobin, "CO₂ waveguide gas laser," *Appl. Phys. Lett.*, vol. 20, pp. 408-410, June 1972.
- [6] J. J. Degnan, H. E. Walker, J. H. McElroy, and N. McAvoy, "Gain and saturation intensity measurements in a waveguide CO₂ laser," *IEEE J. Quantum Electron. (Corresp.)*, vol. QE-9, pp. 489-491, Apr. 1973.
- [7] R. L. Abrams, presented at the Conf. Laser Spectroscopy, Vail, Colo., June 1973.
- [8] P. W. Smith, T. J. Bridges, E. G. Burkhardt, and O. R. Wood, "Mode-locked high pressure waveguide CO₂ laser," *Appl. Phys. Lett.*, vol. 21, pp. 470-472, Nov. 1972.
- [9] V. K. Konyukhov, "Similar gas discharges for CO₂ lasers," *Sov. Phys.—Tech. Phys.*, vol. 15, pp. 1283-1287, Feb. 1971.
- [10] A. von Engel and M. Steenbeck, *Elektrische Gasentladungen, Ihre Physik und Technik*. Berlin, Germany: Springer, 1934.
- [11] E. I. Gordon and A. D. White, "Similarity laws for the effects of pressure and discharge diameter on gain of He-Ne lasers," *Appl. Phys. Lett.*, vol. 3, p. 199, Dec. 1963.
- [12] A. Yariv, *Quantum Electronics*. New York: Wiley, 1967, p. 243.
- [13] R. L. Abrams, "Coupling losses in hollow waveguide laser resonators," *IEEE J. Quantum Electron.*, vol. QE-8, pp. 838-843, Nov. 1972.
- [14] A. N. Chester and R. L. Abrams, "Mode losses in hollow waveguide lasers," *Appl. Phys. Lett.*, vol. 21, pp. 576-578, Dec. 1972.
- [15] T. F. Deutsch and F. A. Horrigan, "Life and parameter studies on sealed CO₂ lasers," *IEEE J. Quantum Electron. (Corresp.)*, vol. QE-4, pp. 972-976, Nov. 1968.
- [16] C. P. Christensen, C. Freed, and H. Haus, "Gain saturation and diffusion in CO₂ lasers," *IEEE J. Quantum Electron.*, vol. QE-5, pp. 276-283, June 1969.
- [17] H. Kogelnik and T. J. Bridges, "A nonresonant multipass CO₂-laser amplifier," *IEEE J. Quantum Electron. (Corresp.)*, vol. QE-3, pp. 95-96, Feb. 1967.
- [18] I. Simon and H. O. McMahon, "Study of the structure of quartz, cristobalite, and vitreous silica by reflection in infrared," *J. Chem. Phys.*, vol. 21, pp. 23-30, Jan. 1953.
- [19] E. Loh, "Optical phonons in BeO crystals," *Phys. Rev.*, vol. 166, pp. 673-678, Feb. 15, 1968.
- [20] H. G. Häfele, "Das Infrarotspektrum des Rubins," *Z. Naturforsch. A*, vol. 18, pp. 331-335, Mar. 1963.

Magnitude and Dispersion of Kleinman Forbidden Nonlinear Optical Coefficients

BARRY F. LEVINE

Abstract—Starting with a perturbation expansion for the Kleinman forbidden nonlinear optical coefficient d_{ijk}^F and for Miller's Δ_{ijk}^F , and making several approximations, we arrive at a simple result for the ratio of forbidden to allowed mixing nonlinearities ($\omega_1 + \omega_2 = \omega_3$), namely $\Delta_{ijk}^F/\Delta_{ijk}^A \propto (\omega_3^2 + 2\omega_1\omega_2)$. For second-harmonic generation (SHG) this can be expressed as $\Delta_{ijk}^F/\Delta_{ijk}^A \approx (\omega/\chi)(\partial\chi/\partial\omega)$, which clearly shows the close connection between Δ_{ijk}^F and the linear dispersion. These expressions are shown to give good agreement with literature experimental values, as well as for our measurements on TeO₂ for various input frequencies ω_1 and ω_2 (i.e., $\omega_3 = 1.88, 2.33, 2.82, 3.50$, and 3.76 eV).

I. INTRODUCTION

RECENTLY [1]-[3], there have been several measurements of Kleinman [4] forbidden nonlinear optical coefficients d_{ijk}^F , i.e., those that would vanish if the Kleinman symmetry [4] relation were strictly valid. The magnitude and origin of these nonzero coefficients is well known [5], [6] to be closely related to the dispersion of the refractive indices. That is, for dispersionless and lossless media the Kleinman symmetry [4] should hold exactly. Franken and Ward [5], [6] have shown (using a quantum

mechanical perturbation expansion) that this dispersion is in fact large enough to explain the order of magnitude of these forbidden coefficients. In this paper we show that by using a similar model we can quantitatively explain these recent measurements [1]-[3] as well as earlier results [7]-[9] for d_{ijk}^F . We also present some new theoretical and experimental results on the dispersion of these forbidden coefficients.

It is interesting to note here that the familiar anharmonic oscillator model [10] predicts the well-known result that Miller's delta [9] $\Delta_{ijk} = d_{ijk}/\chi_i\chi_j\chi_k$ is independent of frequency. Because of this complete lack of dispersion, the Kleinman symmetry condition [4] is strictly true for this model, and hence the Kleinman forbidden coefficients are exactly zero. This is also the case for the bond-charge model [11]. Thus we must use a more accurate model for Δ_{ijk}^F in order to predict its magnitude and dispersion.

II. THEORY

It is well known [12] that a perturbation expansion for the nonlinear susceptibility d_{ijk} for sum frequency generation $\omega_1 + \omega_2 = \omega_3$ yields the following expression